JCSE The Journal of Corrosion Science and Engineering

21st Century Corrosion Science

Volume 6 Paper C013

Electrochemical Corrosion Behavior of Tubing Alloys in Simulated Space Shuttle Launch Pad Conditions

L. M. Calle[1], R.D. Vinje[2], and L.G. MacDowell[1]

[1] *NASA, Mail Code YA-F2-T, Kennedy Space Center, FL 32899, USA, Luz.M.Calle@nasa.gov*

[2] *ASRC Aerospace, Mail Code ASRC-15, Kennedy Space Center, FL 32899, USA*

Abstract

At the Kennedy Space Center, NASA relies on stainless steel (SS) tubing to supply the gases and fluids required to launch the Space Shuttle. 300 series SS tubing has been used for decades but the highly corrosive environment at the launch pad has proven to be detrimental to these alloys. An upgrade with higher alloy content materials has become necessary in order to provide a safer and long lasting launch facility. In the effort to find the most suitable material to replace the existing AISI 304L SS (UNS S30403) and AISI 316L SS (UNS S31603) shuttle tubing, a study involving atmospheric exposure at the corrosion test site near the launch pads and electrochemical measurements is being conducted.

This paper presents the results of an investigation in which stainless steels of the 300 series, 304L, 316L, and AISI 317L SS (UNS S31703) as well as highly alloyed stainless steels 254-SMO (UNS S32154), AL-6XN (N08367) and AL29-4C (UNS S44735) were evaluated using direct current (DC) electrochemical techniques in three different electrolyte solutions. The solutions consisted of neutral 3.55% NaCl, 3.55% NaCl in 0.1N HCl, and 3.55% NaCl in 1.0N HCl. These solutions were chosen to simulate an environment that is less, similar, and more aggressive respectively than the conditions at the Space Shuttle launch pads.

This paper was presented at the Conference "Corrosion Science in the 21st Century" held at UMIST in July 2003.

The electrochemical results were compared to the atmospheric exposure data and evaluated for their ability to predict the long-term corrosion performance of the alloys.

Keywords: 304L, 316L, 317L, 254-SMO, AL-6XN, AL29-4C, stainless steel, acidic NaCl, DC measurements, atmospheric exposure.

Introduction

304L stainless steel (304L SS) tubing is used in various supply lines that service the Orbiter at the Kennedy Space Center (KSC) launch pads. The atmosphere at the launch site has a very high chloride content caused by the proximity of the Atlantic Ocean. During a launch, the exhaust products from the fuel combination reaction in the solid rocket boosters produces hydrochloric acid. The acidic chloride environment is aggressive to most metals and causes severe pitting in some of the common stainless steel alloys. 304L SS tubing is susceptible to pitting corrosion that can cause cracking and rupture of both high-pressure gas and fluid systems.1 The failures can be life threatening to launch pad personnel in the immediate vicinity. Outages in the systems where the failure occurs can create schedule impact to normal operation and shuttle launches. The use of a better tubing alloy for launch pad applications would greatly reduce the probability of failure, improve safety, lessen maintenance costs, and reduce downtime losses. The objective of this work was to study the electrochemical behavior of corrosion resistant tubing alloys to replace the 304L SS tubing at the Space Shuttle launch sites. The stainless steel alloys chosen for this investigation were: 304L, 316L, 317L, AL-6XN, AL29-4C and 254 SMO. 304L SS was included in the study for comparison purposes. These alloys were tested in three different electrolytes that provided less severe, similar, and more aggressive conditions than those found at the launch pads at the Kennedy Space Center in Florida (USA).

Materials and Methods

Alloys

Table 1 lists the tubing alloys chosen for this investigation. Table 2 lists trade name, UNS number, and chemical composition of each material. The specimens were flat sample coupons, 3.2 cm in diameter, from Metal Samples Co. The test specimens were polished to 600-grit, ultrasonically degreased in a detergent solution, and wiped with acetone before testing.

TABLE 1

Alloys

Alloy	Class
304L	Low carbon austenitic stainless steel
316L	Molybdenum-containing austenitic stainless steel
317L	Molybdenum-containing austenitic stainless steel
AL-6XN	Superaustenitic stainless steel
AL29-4C	Superferritic stainless steel
254 SMO	Austenitic stainless steel

Experimental

A model 352 SoftCorr™ III Corrosion Measurement System, manufactured by EG&G Princeton Applied Research, was used for all electrochemical measurements. The equipment includes the software that is designed to measure and analyze corrosion data. The electrochemical cell (flat cell) included a saturated calomel reference electrode (SCE), a platinum-on-niobium counter electrode, the working electrode, and a bubbler/vent tube. The specimen holder in the cell is designed such that the exposed metal surface area is 1 cm^2.

TABLE 2

Chemical Composition of Stainless Steels Alloys

Alloy	304L	316L	317L	AL-6XN	AL29-4C	254 SMO
UNS Number	S30403	S31603	S31703	N08367	S44735	S31254
Fe	71.567	69.053	63.525	48.118	66.594	55.162
Ni	8.200	10.140	13.200	23.88	0.260	17.900
Cr	18.33	16.240	18.100	20.470	28.750	20.000
Mo	0.500	2.070	3.160	6.260	3.780	6.050
Mn	1.470	1.780	1.510	0.300	0.260	0.490
C	0.023	0.019	0.017	0.020	0.020	0.012
N	0.030	0.050	0.030	0.330	0.031	0.196
Si	0.380	0.280	0.460	0.40	0.280	0.350
P	0.030	0.027	0.027	0.021	0.023	0.019
s	0.0002	0.001	0.001	0.0003	0.002	0.001
Cu	0.460	0.340	0.150	0.200		0.680
Co		0.240				
Nb					0.290	
Ti					0.360	

Three different aerated electrolyte solutions were used: (1) 3.55% NaCl, (2) 3.55% NaCl-0.1N HCl and (3) 3.55% NaCl-1.0N HCl. These solutions emulate less than, similar to, and more aggressive conditions than those found at the launch pads at KSC.

Corrosion potential, linear, and cyclic polarization data were gathered for the alloys under the three different electrolyte conditions. Polarization resistance determinations were generally based on ASTM G59. Cyclic polarization data were gathered using ASTM G 61as a guideline. Duplicate and triplicate tests had essentially the same outcome. The reported results are the averages of two or more runs.

The corrosion potential was monitored until the sample reached a potential that was stable within ±5 mV for a period of 10 minutes. Linear polarization measurements were performed immediately after. A potential range of ±20 mV versus open circuit potential was used for these measurements. The scan rate was 0.166 mV/sec. A linear graph of potential (E) versus current (I) was obtained and the polarization resistance (R_p) calculated.

Cyclic polarization measurements were started at –250mV relative to the corrosion potential (E_{corr}). The scan rate was 0.166mV/sec. The scans were reversed when the current density reached 5mA/cm^2. The reverse potential scan continued until the potential returned to the starting potential of –250 mV relative to E_{corr}. A graph of E versus Log (I) was obtained. From this graph, the breakdown potential (E_{bd}), repassivation potential (E_{rp}), and the area of the hysteresis loop were obtained. Linear and cyclic polarization results were calculated using the SoftCorr III software.

Atmospheric Exposure

A beach atmospheric exposure site near the launch pads was used to evaluate the performance of the six alloys included in this study for their resistance to localized corrosion under atmospheric conditions similar to those at the launch pad. Three tubes of each alloy were exposed. A 10 percent (v/v) solution of HCl and 28.5 grams of alumina powder per 500 ml of solution was mixed into acid slurry to simulate solid rocket booster deposition. One set of tubes was sprayed every two weeks with the acid slurry to accelerate the corrosion effect. The other set was left exposed to the natural marine seacoast environment.

Results and Discussion

Corrosion Potential

Corrosion potential gives an indication of how noble a metal is in a given environment. In general, a more positive corrosion potential means that the metal can be expected to be more resistant to corrosion in that particular electrolyte than one with a more negative corrosion potential. Thus, most metals can be ranked according to resistance to corrosion based on corrosion potential. Stainless steels, as passive materials, can fluctuate from an active to passive state depending on the environment to which they are exposed, the velocity of the solution, and passivation treatments applied during manufacturing.

The corrosion potential for each alloy was monitored from the initial time of immersion until a stable potential was observed. The alloys differed in the time it took for the potential to stabilize. For simplicity, Figure 1 shows only the open circuit potential for the SS alloys at times just prior to and during stabilization. Table 3 lists the average value of the stable open circuit potential. Contrary to what was expected based on the composition of the alloys, the highly alloyed SS 254-SMO, AL6XN and AL29-4C did not exhibit a more noble stable potential when compared to 316L and 317L in 3.55% NaCl (Figure 1a). This behavior did not correlate with the performance of the tubing samples exposed to the atmosphere at the corrosion test site. As it was expected, 304L was the most active alloy in this environment with a stable corrosion potential of -173 mV vs. SCE. In 3.55% NaCl-0.1N HCL, the three highly alloyed SS displayed a more noble potential than the 300 series SS as it was expected based on their composition. This behavior became more pronounced when the concentration of HCl in the 3.55% NaCl solution was increased to 1.0N. Figure 1c shows a clear distinction between the more noble behavior of the highly alloyed SS in the 3.55% NaCl-1.0N HCl and the more

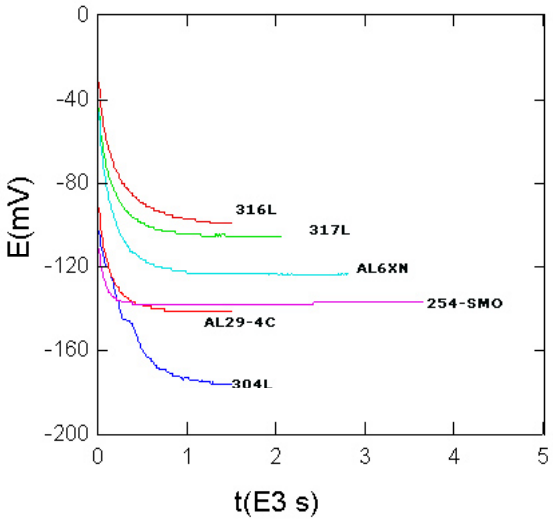
0
-40
-80
-120
-160
-200
E(mV)
0
1
2
3
4
5
t(E3 s)
316L
317L
AL6XN
254-SMO
AL29-4C
304L

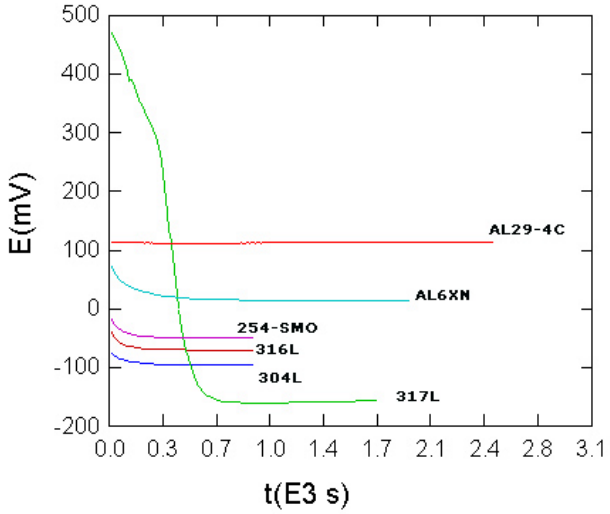
500
400
300
200
100
0
-100
-200
E(mV)
0.0
0.3
0.7
1.0
1.4
1.7
2.1
2.4
2.8
3.1
t(E3 s)
AL29-4C
AL6XN
254-SMO
316L
304L
317L

(a) (b)

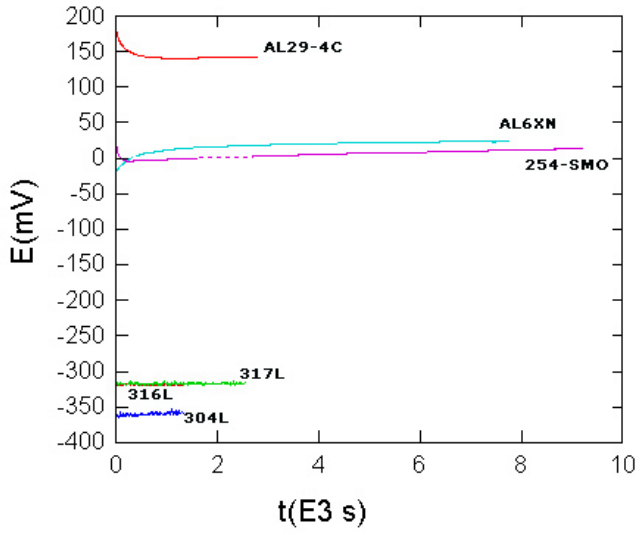
200
150
100
50
0
-50
-100
-150
-200
-250
-300
-350
-400
E(mV)
0
2
4
6
8
10
t(E3 s)
AL29-4C
AL6XN
254-SMO
317L
316L
304L

(c)

FIGURE 1. Corrosion potential of SS Alloys in (a) neutral 3.55% NaCl, (b) 3.55% NaCl-0.1N HCl, and (c) 3.55% NaCl-1.0N HCl.

active behavior of the 300 series SS. The ennoblement of the higher alloyed SS as the concentration of HCl in the 3.55% NaCl solution increased was most

pronounced for AL29-4C (269 mV increase in the corrosion potential) followed by AL-6XN (153 mV increase) and 254 SMO (144 mV increase). This behavior correlated very well with the actual corrosion performance of the alloys under atmospheric exposure. The transition toward a more active corrosion potential of the 300 series SS as the concentration of HCl in the electrolyte increased can be attributed to the fact that these SS are easily attacked by HCl because the passive film is not easily attained.2 Chloride (Cl^-) ions are well known for their ability to attack SS by penetrating the protective layer at any discontinuity of the oxide film. The addition of HCl, a reducing acid, exacerbates the attack by interfering with the formation of the oxide film.3

Polarization Resistance

Figure 2 shows linear polarization plots for SS 316L in 3.55% NaCl with increasing HCl concentrations (neutral (a), 0.1N (b), and 1.0N (c)). It is evident from the figure that the slope of the line is decreases as the acidity of the 3.55% NaCl solution increases. This behavior is indicative of the decrease in the polarization resistance. Table 4 summarizes the polarization resistance, R_p, values in neutral 3.55% NaCl, 3.55% NaCl-0.1N HCl, and in 3.55% NaCl-1.0N HCl for all the alloys. The R_p values show that increasing the HCl concentration in the 3.55% NaCl solution resulted in a significant decrease in the R_p values of the 300 series SS. The decrease in the R_p values, indicative of an increase in the corrosion rate, in the presence of increasing concentrations of HCl, can be attributed to the fact that the protective layer of the 300 series SS becomes unstable. This is illustrated by the drastic decrease in R_p from

1.36 Mohms.cm^2 in neutral 3.55% NaCl to 159 ohms.cm^2 in 3.55%NaCl-1.0N HCl for 316L (Figure 2 and Table 4).

R_p values for AL-6XN, AL29-4C, and 254 SMO in neutral 3.55% NaCl were approximately of the same order of magnitude as those for the 300 series SS. However, the R_p values for these alloys remained high as the concentration of

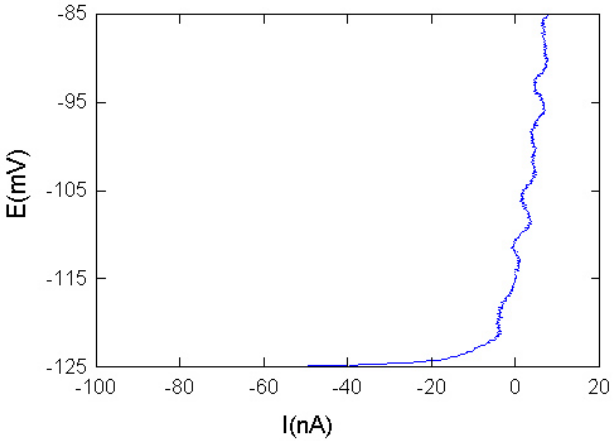

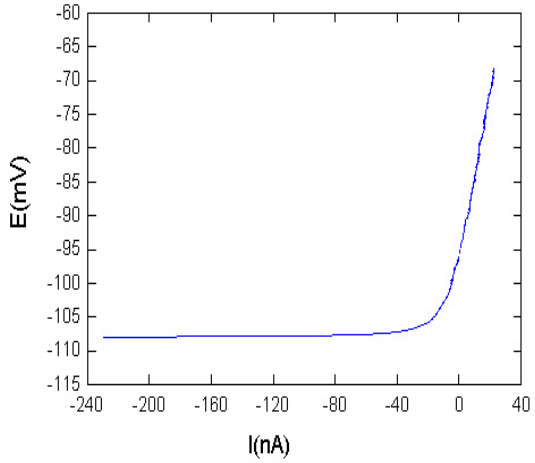

(a) (b)

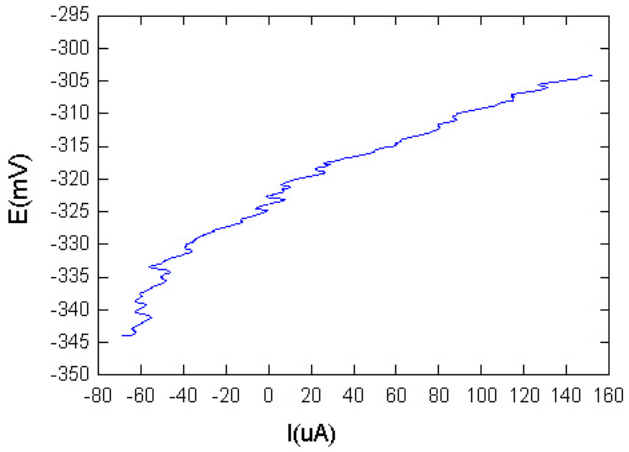

(c)

FIGURE 2. Linear polarization curves for 316L in (a) neutral 3.55% NaCl, (b) 3.55% NaCl-0.1N HCl, and (c) 3.55% NaCl-1.0N HCl.

HCl in the 3.55% NaCl solution increased. AL-6XN and 254 SMO showed a slight decrease in R_p as the concentration of HCl increased while AL29-4C exhibited no change in Rp after the initial slight increase. The lower corrosion rates of AL6XN, AL29-4C, and 254-SMO SS can be attributed to the presence of greater amounts of chromium, nickel and molybdenum that result in a more stable protective layer on the surface of the alloy. The low corrosion rate of AL29-4C, which remained fairly unchanged with the increased concentration of HCl, can be attributed to its high (28.750%) chromium content.

Cyclic Polarization

Cyclic Polarization measurements were performed in order to determine the tendency of the alloys to undergo localized (pitting or crevice) corrosion when placed in the electrolyte solutions. The resulting plot of the potential-current function is strongly indicative of the tendency of the material to undergo localized attack. In effect, the function traces a hysteresis loop, with the area of the loop indicating the amount of localized corrosion of the material. From the area value, it is possible to analyze the performance of the alloys. Hysteresis loop area values should be very small for alloys that are highly resistant to

localized corrosion. In this case, the reverse scan traces almost exactly over the forward scan.4,5

Two important potentials, also used to characterize the hysteresis loop, are the critical breakdown potential, E_{bd}, defined as the potential forward scan "knee" potential. Pitting is characterized by a rapid increase in current with a very small change in potential. Above this potential, pits initiate and propagate. The repassivation potential, E_{rp}, is defined as the point where the reverse scan intersects the forward scan. At this potential, localized attack stops and the current decreases significantly past the passive current density. The more positive the value of E_{bd}, the more resistant the alloy is to initiation of localized corrosion. Also, the more positive the value of E_{rp}, the more resistant the alloy to corrosion. 6 Values of E_{bd} and E_{rp} for the SS alloys in the three different electrolytes are shown in Table 5.

Cyclic polarization scans for three of the alloys included in this investigation are shown in Figures 3-5. Hysteresis loop area values are given in Table 6. Figure 3 shows a cyclic polarization scan for SS AL29-4C in 3.55% NaCl-1.0N HCl. In this case, the reverse scan traced almost exactly over the forward scan resulting in

TABLE 3

Corrosion potentials of SS alloys in neutral 3.55% NaCl, 3.55% NaCl-0.1N HCl, and in 3.55% NaCl-1.0N 3.55% NaCl

Alloy	E_{corr} (mV)		
	Neutral	0.1N HCl	1.0N HCl
304L	-155	-122	-349
316L	-102	-130	-320
317L	-111	-150	-318
AL-6XN	-125	12	28
AL29-4C	-132	110	137

254 SMO	-132	-48	12

no hysteresis. This is characteristic of an alloy that is highly resistant to localized corrosion. Figure 4 shows the overlay of the cyclic polarization scans for SS 316L and SS 254-SMO in 3.55% NaCl-1.0N HCl. The hysteresis loop area values for these two alloys are very similar under these conditions (5.58 and 5.98 coulombs respectively) indicating a high resistant to localized corrosion. However, because of the significance of E_{bd} and E_{rp}, it is important to take also into account the position of the scan in the E vs. Log (I) diagram when analyzing cyclic polarization data. Values for E_{bd} and E_{rp} are shown in Table 6. While the area of the hysteresis loop is very similar (Figure 4), the position of the scans in the plot is very different. The values of E_{bd} and E_{rp} for 316L are -42 mV and -37 mV respectively, while the values for 254-SMO are 877 mV and 890 mV. These results indicate that 254-SMO is a superior alloy in its corrosion resistance to localized corrosion when compared to 316L under the same conditions. Similar results were obtained for AL-6XN and AL29-4C.

TABLE 4

Polarization resistance of SS alloys in 3.55% NaCl in various concentrations of HCl

Alloy	R_p (ohms.cm^2)		
	Neutral	0.1N HCl	1.0N HCl
304L	6.37×10^5	7.05×10^5	2.00×10^2
316L	1.36×10^6	4.80×10^5	1.59×10^2
317L	1.49×10^6	2.99×10^5	1.93×10^2
AL-6XN	1.40×10^6	1.18×10^6	0.615×10^6
AL29-4C	0.882×10^6	1.09×10^6	1.09×10^6
254 SMO	1.08×10^6	1.01×10^6	0.782×10^6

TABLE 5

Critical breakdown potential and repassivation potential for SS alloys 3.55% NaCl in different concentrations of HCl

Alloy	Neutral		0.1N HCl		1.0N HCl	
	E_{bd} (mV)	E_{rp} (mV)	E_{bd} (mV)	E_{rp} (mV)	E_{bd} (mV)	E_{rp} (mV)
304L	366	-136	167	-153	-60	-58
316L	380	-143	135	-164	-42	-37
317L	622	-131	432	-91	-90	-89
AL-6XN	922	906	816	835	902	904
AL29-4C	964	964	818	N/A	878	N/A
254 SMO	952	939	825	831	877	890

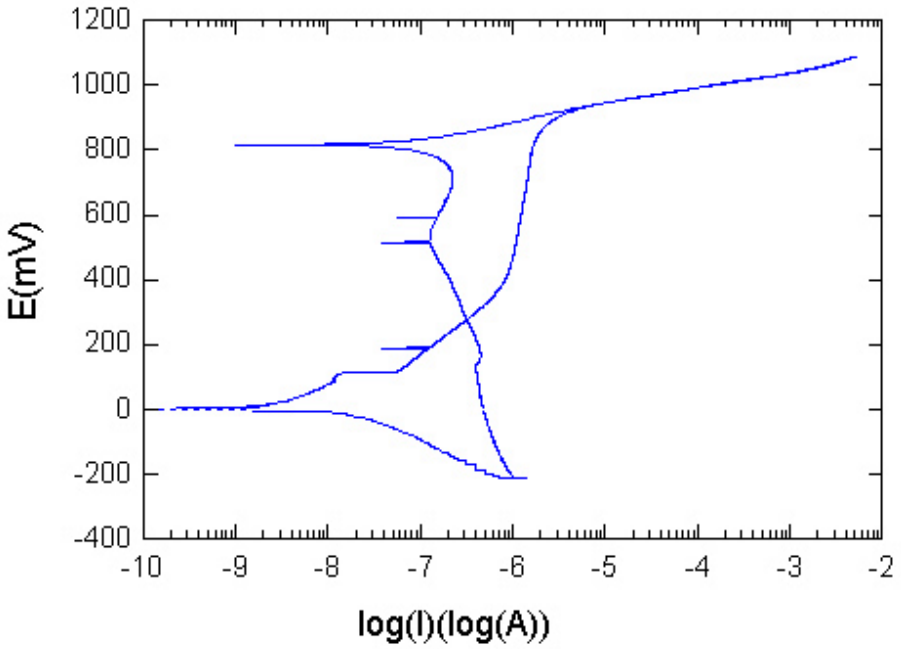

FIGURE 3. Cyclic polarization for AL29-4C in 3.55% NaCl-1.0N HCl

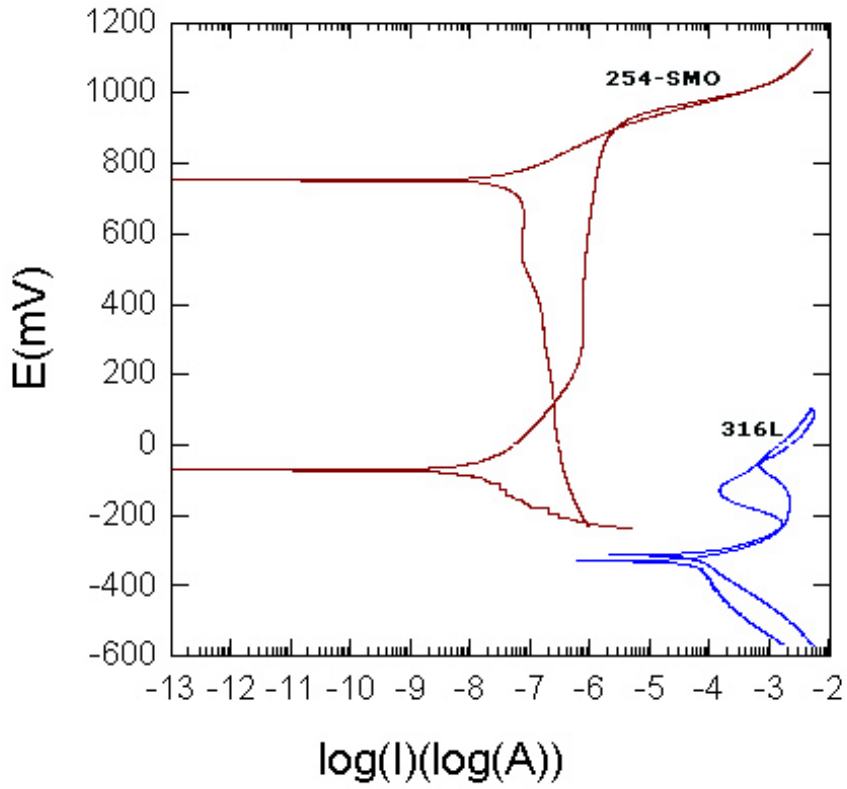

FIGURE 4. Cyclic polarization for 316L and 254-SMO in 1.0N-HCl 3.55% NaCl

SS AL29-4C is an alloy very resistive to localized corrosion as indicated by the very small hysteresis loop area in the cyclic polarization scan obtained in neutral 3.55% NaCl. The increase in the acid concentration of the 3.55% NaCl
solution to 0.1N resulted in a negative hysteresis. A further increase to 1.0N in the concentration of the acid resulted in no hysteresis (Figure 3). SS AL-6XN and 254 SMO exhibited small hysteresis loop areas in the three electrolytes indicative of their resistance to localized corrosion in neutral and acidic 3.55% NaCl.

Figure 5 shows the effect of increasing HCl concentration on the cyclic polarization scans of SS 304L. The scan in neutral 3.55% NaCl solution displays a higher corrosion potential as well as lower current density. When the HCl concentration was increased to 0.1N, the corrosion potential became more negative and the current density increased. The metal still portrays passive behavior where the voltage increases with small changes in current density. However, increasing the acid concentration to1.0N HCl affects the alloy more drastically. Past the

corrosion potential, the material experiences anodic dissolution and then repassivates over a small voltage range and rapidly experiences breakdown of the passive film at E_{bd}. Similar behavior was observed for the other 300 series SS. For these alloys, a decrease in the hysteresis loop area cannot be interpreted as an indication of increased resistance to localized corrosion.

A decrease in the difference between E_{corr} and E_{bd} has been associated with increased susceptibility to localized corrosion.7 Table 6 shows the values for the difference between E_{corr} and E_{bd} for the SS alloys in the three different electrolytes. The values for the 300 series SS are lower than those for the higher alloyed materials and their decrease as the concentration of acid in the electrolyte increases is greater than for the higher alloyed materials. These results are in agreement with results from visual observations of the samples as well as with the atmospheric exposure data on the susceptibility to localized corrosion of these alloys.

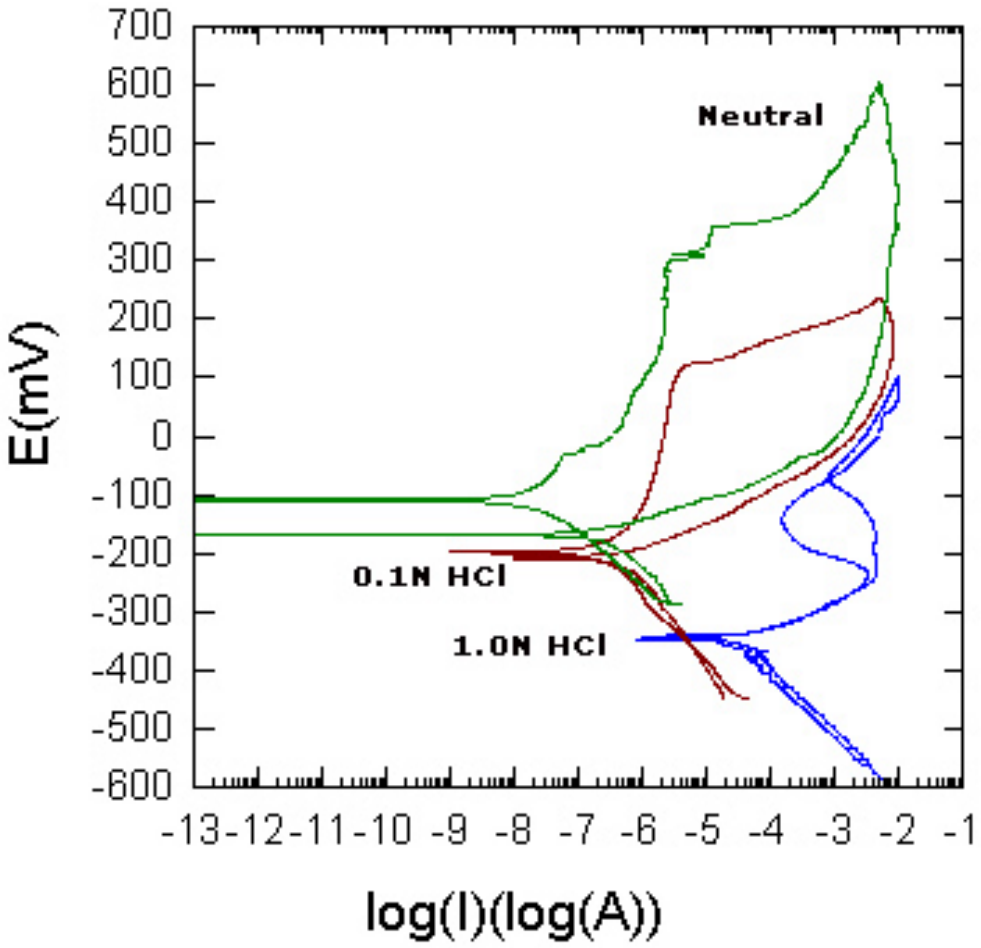

FIGURE 5. Cyclic polarization scans for 304L in neutral, 0.1N and 1.0N HCl–3.55% NaCl solutions

Pitting Resistance Equivalent Number

It is well established that the pitting corrosion resistance of stainless steels depends mainly upon their chromium, molybdenum, and nitrogen contents. This resistance is evaluated empirically through the pitting resistance equivalent number (PREN) defined as

$$PREN = (\%Cr) + (3.0) \times (\%Mo) + (15) \times (\%N)$$

where the percentage corresponds to the weigh percentage of the element in the alloy.[8,9,10] PREN numbers for the alloys investigated are shown in Table 8. These values are in good agreement with the experimental results.

TABLE 6

Area of hysteresis loop for SS alloys in 3.55% NaCl with various concentrations of HCl

Alloy	Area of Hysteresis Loop (coulombs)		
	Neutral	0.1N HCl	1.0N HCl
304L	22.96	11.36	10.42
316L	15.99	12.35	5.58
317L	33.12	23.53	12.58
AL-6XN	5.07	3.23	1.69
AL29-4C	5.23	Negative Hysteresis	No Hysteresis
254 SMO	5.11	4.85	5.98

TABLE 7

Difference between E_{corr} and E_{bd} for SS alloys in 3.55% NaCl with different concentrations of HCl

Alloy	$E_{bd}-E_{corr}$ (mV)		
	Neutral	0.1N HCl	1.0N HCl
304L	514	401	287
316L	510	424	271
317L	810	730	221
AL-6XN	1081	895	950
AL29-4C	1129	757	746
254 SMO	1106	978	944

TABLE 7

PREN numbers for stainless steel alloys

Alloy	304L	316L	317L	AL-6XN	AL29-4C	254 SMO
PREN	19	26	31	46	40	43

Atmospheric Exposure

The most important criteria of any laboratory test for localized corrosion is that it must rate alloys consistently with service performance in environments that cause localized corrosion. In this study, the laboratory results were compared to the two-year atmospheric exposure data. Detailed results of the atmospheric exposure have been previously reported elsewhere.11 Photographs of the tubes after one year of atmospheric exposure with no acid rinse are shown in Figure 5. Photographs of the tubes after two years of atmospheric exposure with biweekly acid rinse are shown in Figure 6. A photograph of SS 304L is not shown because the tube failed prior to the two-year evaluation and was removed from the test rack. A summary of the visual evaluation of the tubing test articles after two years of atmospheric exposure is summarized in Table 8.

TABLE 8

Visual observations of tube specimens after two years of atmospheric exposure

Visual Observations after Two Years of Atmospheric Exposure		
Alloy	Natural	With Acid-Alumina Slurry Rinse
304L	Tubes in poor condition with pits and brown spots all over	Tubes failed due to pitting. Pits went through the thickness of the tube
316L	Tubes in poor condition with pits and brown stains. Better than 304L	2 out 3 tubes failed. Remaining tube in bad condition with brown spots and pits all over
317L	Brown spots and pits on the tube. Better than 316L	1 out 3 tubes failed. Pits and brown spots all over the tube. Better condition than 316L
AL-6XN	Light browning of the tube.	Tubes look in good condition with slight discoloration
AL29-4C	Slight discoloration of the tubes. Over all in good condition.	Tubes in good condition
254-SMO	Tube is in good condition. Some spots along the seam weld	Tubes look very good except for pits on the seam weld

304L

316L

317L AL29-4C

FIGURE 5. Tubing after two years of natural seacoast atmospheric exposure (no acid rinse.

FIGURE 5. Photographs of tubing sections after two years of seacoast atmospheric exposure with acid rinse every two weeks.

Conclusions

Electrochemical measurements of the six alloys indicated that the higher alloyed SS 254 SMO, AL29-4C, and AL-6XN exhibited a significantly higher resistance to localized corrosion than the 300 series SS.

The stable corrosion potential values obtained in neutral 3.55% NaCl did not correlate with the performance of the alloys under natural seacoast atmospheric exposure.

A correlation was found between the stable corrosion potential values obtained in acidic 3.55% NaCl and the corrosion performance of the alloys under atmospheric exposure with and without acid rinse.

There was a correlation between the corrosion performance of the alloys during the two year atmospheric exposure and the corrosion rates based on polarization resistance values.

The area of the hysteresis loop cannot be used as the sole criterion to predict susceptibility to localized corrosion.

There was a correlation between the atmospheric exposure data and the susceptibility to localized corrosion that was predicted based on the difference between E_{bd} and E_{corr}. These predictions were in agreement with the expectations based on the PREN calculated for the alloys.

References

1 S. McDanels, Failure Analysis of Launch Pad Tubing, Microstructural Science, **25**, p. 125-129 (1998).

2 Metals Hanbook, 13, p. 557, (ASM International, Metals Park, OH, 1987).

3 N.G. Thompson and J.H. Pager, DC electrochemical Test Methods, p. 57, (Houston, TX: NACE International, 1986).

4 W.S. Tait, Corrosion, 34 (6) (1978): pp.214-217.

5 W.S. Tait, corrosion, 35 (7) (1979): pp. 296-300.

6 Z. Szklarska-Smialowska, M. Janik-Czacho, Corros. Sci. 11 12(1971): p. 901.

7 J. Beddoes and J. Gordon Parr, Introduction to Stainless Steels (ASM International, Materials Park, OH, 1999, p. 83.

8 M.J. Matthews, Metall. Mater. Technol. 5 (1982): p. 205.

9 C.A. Clark, P. Gentil, P. Guha, "Development of Improved Alloy Duplex Steel, ed. J. Van Liere (The Hague, The Netherlands: Netherlands instituut Voor Lastechniek, 1986).

10 A.J. Sedriks, Corrosion 42, 7 (1986): p. 376.

11 R.G. Barile, L.G. MacDowell, J. Curran, L.M. Calle, and T. Hodge, "Corrosion of Stainless Steel tubing in a Spacecraft Launch Environment," Paper No. 02152, Corrosion/2002, 57th Annual Conference & Exposition, April 7-11, 2002, Denver, Colorado.